Int. J. Heat Mass Transfer. Vol. 24, pp. 521–531
© Pergamon Press Ltd. 1981. Printed in Great Britain

0017-9310/81/0301-0521 $02.00/0

MEASUREMENTS OF CHARACTERISTIC TIME SCALES OF THE TURBULENT BOUNDARY LAYER WITH MASS TRANSFER

E. ALP

Analysis and Modelling, Atomic Power Division, Westinghouse Canada Limited, Hamilton, Ontario, Canada

and

A. B. STRONG

Mechanical Engineering Department, University of Waterloo, Waterloo, Ontario, Canada

(*Received* 4 *April* 1979 *and in revised form* 20 *August* 1980)

Abstract—The results of an experimental survey on the transpired turbulent boundary layer with constant pressure and blowing fraction are reported in the present paper. The working fluid was air at atmospheric pressure. Characteristic time scales of the near-wall region were measured as well as mean velocity profiles and turbulence parameters using constant temperature hot-wire anemometry. Integral parameters of the boundary layer and local friction factors are also presented. Comparisons are made with earlier studies.

The outer portion of the mean velocity profiles $U^+(y^+)$ seems to be more affected with blowing than the near-wall portion. The region of maximum turbulence fluctuations moves away from the wall with blowing, indicating that the length scale and thus the time scale of fluctuations near the wall are increased. This is consistent with the findings on the characteristic time scale T_B. The characteristic time scale parameter $\bar{T}_B$ is found to correlate well with the mass-transfer parameter V_w^+.

NOMENCLATURE

A, van Driest's constant [m];
A^+, Au_τ/ν;
B, blowing parameter, $= V_w^+(C_f/2)^{1/2}$;
C_f, friction factor, $\equiv \tau_w/(\frac{1}{2}\rho U_G^2)$;
e, fluctuating anemometer voltage output;
e^2, RMS of fluctuating anemometer voltage output;
E, time averaged hot-wire anemometer voltage output;
$\tilde{E}$, instantaneous anemometer voltage output, $\tilde{E} = E + e$;
$f(V_w^+)$, dimensionless function defined by equation (2);
f_B, mean frequency of "bursts" [s^{-1}];
G, Clauser's shape factor, $\equiv \Delta_2^+/\Delta_1^+$;
H, shape factor, $\equiv \delta_1/\delta_2$;
l_m, mixing length [m];
l_m^+, $l_m u_\tau/\nu$;
$q^2/2$, kinetic energy of turbulence,

$$\equiv (\overline{u^2} + \overline{v^2} + \overline{w^2})/2 \ [m^2/s^2];$$

$R_{11}(\tau_i)$, autocorrelation coefficient,

$$\equiv \overline{u(t)u(t+\tau_i)}/\overline{u^2};$$

Re_x, $U_G x/\nu$;
Re_{δ_2}, $U_G \delta_2/\nu$;
t, time coordinate [s];
T_B, mean period of turbulent "bursts" in the viscous sublayer [s];
T^+, dimensionless time parameter, $\equiv Tu_\tau^2/\nu$;
T^*, dimensionless time parameter, $\equiv TU_G/\delta_1$;
$\bar{T}$, dimensionless time parameter, $\equiv TV_w^2/\nu$;
u, fluctuating velocity in the x direction at y [m/s];
u_τ, friction velocity, $(\tau_w/\rho)^{1/2}$ [m/s];
$\overline{u_i u_j}$, time averaged velocity correlations, u_i, u_j;
U, time averaged velocity in the x direction at y,

$$\equiv \lim_{T\to\infty} \frac{1}{T} \int_{t_0}^{t_0+T} \tilde{U}\,dt \ [m/s];$$

$\tilde{U}$, instantaneous velocity, $\tilde{U} = U + u$ [m/s];
U_G, free stream velocity [m/s];
U^+, dimensionless velocity, $\equiv U/u$;
U^*, dimensionless velocity, $\equiv U/U_G$;
v, fluctuating velocity in the y direction at y [m/s];
V_w, velocity of fluid at the wall in the y-direction [m/s];
V_w^+, dimensionless transpiration velocity,

$$\equiv V_w/u_\tau = B(C_f/2)^{1/2};$$

V_w^*, dimensionless transpiration velocity, $\equiv V_w/U_G$;
w, fluctuating velocity in the z direction [m/s];
x, distance in the direction of main flow [m];
x^+, dimensionless distance, $\equiv xu_\tau/\nu$;
y, distance in the direction perpendicular to wall [m];
y^+, dimensionless distance, $\equiv y_\tau u/\nu$;
z, distance in the direction perpendicular to the xy plane [m].

Greek symbols

β, ratio of "burst" buildup time to the total period;

δ, boundary layer thickness where $U = 0.99U_G$ [m];

δ_1, displacement thickness $\equiv \int_0^\infty \left(1 - \frac{U}{U_G}\right) dy$ [m];

δ^*, $\frac{U_G \delta_1}{\nu}$;

δ_2, momentum thickness $\equiv \int_0^\infty \frac{U}{U_G}\left(1 - \frac{U}{U_G}\right) dy$ [m];

Δ_1^+, $\equiv \int_0^\infty (U_G^+ + U^+) dy^+$;

Δ_+^2, $\equiv \int_0^\infty (U_G^+ - U^+)^2 dy^+$;

κ, Prandtl's mixing length constant;

μ, dynamic viscosity [kg/(m/s)];

ν, kinematic viscosity [m^2/s];

ρ, density [kg/m^3];

τ_w, wall shear stress $\mu \frac{\partial U}{\partial y}_{y=0}$ [N/m^2];

ψ^+, dimensionless velocity parameter $\equiv \frac{2U^+}{(1 + V_w^+ U^+)^{1/2} + 1}$;

ψ_G^+, ψ^+ evaluated with $U^+ = U_G^+$;

ω, frequency [s^{-1}].

1. INTRODUCTION

THE IMPORTANCE of the near-wall region of a boundary layer, also called the viscous sublayer, has been pointed out in earlier studies by Kim *et al.* [1], and by Kays and Moffat [2] who state, "The 'sublayer', though comprising a very small fraction of the total boundary layer thickness, is the region where the major change in velocity takes place, and, except for very low Prandtl number fluids, is the region wherein most of the resistance to heat transfer resides. If this region is modelled accurately, only a very approximate scheme is needed throughout the rest of the boundary layer".

Recent observations show the presence of turbulent "bursts" in the sublayer, with relatively quiet periods in between them [3–9]. It is conceived that a viscous layer grows on the wall until such time that it becomes unstable, and violently breaks down, forming "streaks" extending into the upper layer of the flow. The extent of the sublayer is not well defined, mainly because a practical and physically viable criterion is lacking to measure its thickness directly. Yet, in the ever popular mixing length models to calculate the turbulent boundary layer, the most commonly employed empirical parameter A^+ [2, 10, 11] is generally interpreted as the characteristic thickness of the sublayer. This parameter, attributed to van Driest [12], must be inferred from mean velocity profile data and cannot be measured directly.

There are other scales of the sublayer, which lend themselves more readily to direct measurement than the above mentioned length scale; and these are time scales. One of them is the mean period T_B of turbulent "bursts". Another parameter which can be observed in principle, but for which quantitative data are not available at present is the ratio β of burst buildup time to the total period. In view of the observation that the breakdown is very rapid [3], this ratio should be nearer to 1 than 0.

Investigations of the transpired boundary layers have shown that the mixing length distribution in the boundary layer is significantly modified by mass transfer [2, 13]. This leads to the belief that mass transfer would influence the "bursting" structure of the near wall region. Thus the primary purpose of the present study is to examine the characteristic time scales of this "bursting" structure in the aforementioned region of a two-dimensional boundary layer with blowing.

In a study of this type, the flow field in which the near-wall measurements are made must be well characterized in terms of the distributions of mean velocity and fluctuating velocity correlations throughout the boundary layer, as well as the wall shear stress and other integral parameters of the flow. These enable us to make meaningful comparisons of different studies and also pave the way for further analysis. Thus the present study includes these required data on the flow field. Some of these data are confirmatory in nature and are felt to be useful, considering the scarcity of accurate experimental data from well confirmed wind tunnels [14, 15]. Other data such as the fluctuating velocity correlations, are believed to be entirely new in the ranges of flow parameters considered here.

2. EXPERIMENTAL APPARATUS

The experimental apparatus used in the present study is the Heat and Mass Transfer Tunnel at the University of Waterloo. The original commissioning of the wind tunnel and the techniques used to ensure two-dimensionality of the flow were described by Watts [14] and Watts *et al.* [15]. In the present experimental program, DISA hot-wire anemometry systems were used for the measurements of "burst" periods and velocities, and, wall shear stress was measured by Preston tubes calibrated by a floating element [16].

2.1. *Measurement method for the mean velocities and velocity correlations*

DISA single hot-wire probes were used to measure the mean velocity profiles $U(y)$, and the turbulence

intensities, $(\overline{u^2})^{1/2}$. The wire was kept parallel to the wall and perpendicular to the mainstream direction. DISA x-wire probes were used to measure the other fluctuating quantities. Two sets of profiles were taken with the x-wire probes: one with the wires in the xy-plane (vertical probe system), the other with the plane of the wires at an angle of 45° to the xy-plane ("banked" probe system). The merits of a "banked" probe system were discussed by Brundrett and Watts [17]. However, the method was found to have some drawbacks in flows where the shear layer is thin relative to the size of the probe [18]. In the present study, the vertical probe system was used to measure the two turbulence intensities $\overline{u^2}$ and $\overline{v^2}$, and also the turbulent shear stress $-\overline{uv}$. The "banked" probe system was used to measure the kinetic energy of turbulence $q^2/2$. The calibration of the hot-wires were made against pitot tubes placed in the free-stream portion of the wind tunnel and by varying the free-stream velocity.

2.2. *Measurement method for time scales*

From the literature, three different methods of estimating "burst" frequencies are apparent (apart from the flow visualization techniques of Kline *et al.* [3], and Corino and Brodkey [4] and highly refined triggering techniques of Lu, Willmarth [6] and Heidrick *et al.* [8]). One is due to Rao *et al.* [5], which involves visual counting of violently active regions obtained on a time plot of differentiated and filtered hot-wire signals. This procedure was also used by Ueda and Hinze [7]. This last reference also suggests that the burst frequency would be detectable on frequency spectra plots of $(\partial\tilde{U}/\partial t)^2$ and $(\partial^2\tilde{U}/\partial t^2)^2$. The third method suggested in the literature is using a plot of the auto-correlation coefficient [1]. The idea is that a violent activity of relatively large period imposed on the "continuous" higher frequency turbulence fluctuations would be detectable as a peak in the auto-correlation coefficient $R_{11}(\tau_i)$ after the initial decay. Recently, Badri Narayanan and Marvin [9] also used this technique to determine characteristic "burst" periods at large Reynolds numbers.

In the present study, the last two of these methods were employed extensively, although the first was also used initially. The schematic diagram of the hot-wire instrumentation used to measure the characteristic "burst" periods is shown in Fig. 1. The single wire probe was kept at a distance of $y \simeq 0.13$ mm from the smooth porous wall. Ten repeated measurements of T_B were made each with the frequency analyzer and the correlator. The measurements were averaged to arrive at the final value of T_B reported in this paper for a particular Reynolds number and blowing fraction.

3. EXPERIMENTAL RESULTS

3.1. *Wall shear stress*

All measurements of wall shear stress were made by

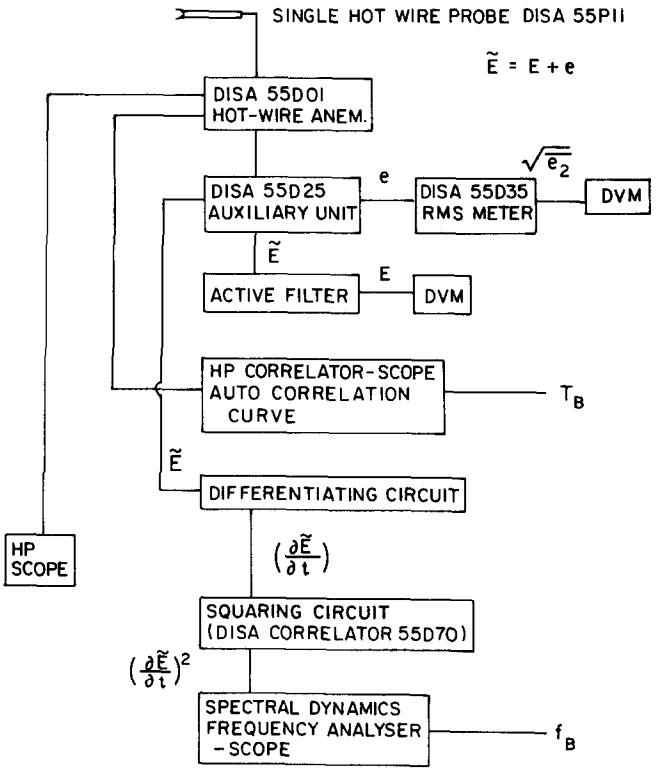

FIG. 1. Schematic of the hot-wire (single) instrumentation.

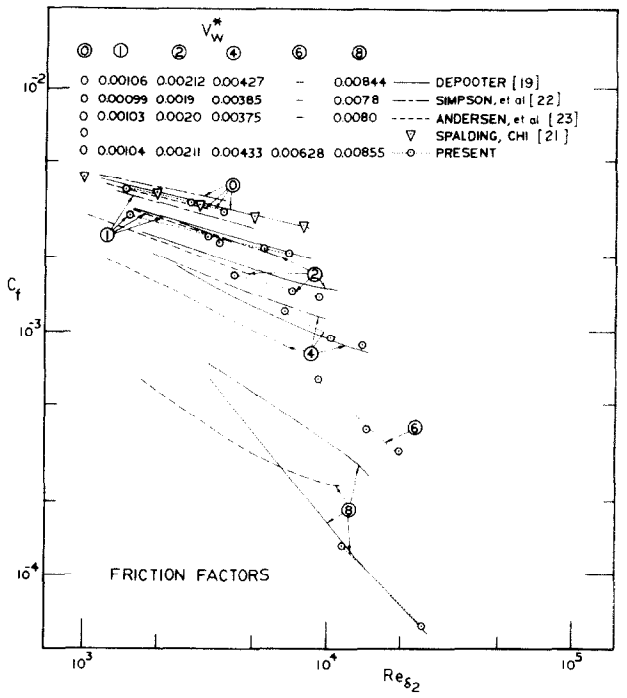

FIG. 2. Friction factor, C_f vs Re_{δ_2}.

Preston tubes, with the exception of the highest blowing rate, for which data were taken from Depooter's $C_f(Re_x)$ results [19]. The Preston tubes used in the present study were calibrated against a floating element under both suction and blowing conditions [16]. The results of the present measurements are plotted in Fig. 2. C_f decreases drastically by increasing blowing and increasing Reynolds number. The uncertainty in the values of C_f is estimated to be between ± 10 and $\pm 20\%$, with the uncertainty increasing with increasing blowing. The uncertainty in the friction velocity u_τ is estimated to vary between $\pm 7\%$ for flat plate and $\pm 15\%$ for high blowing (calculated using the Kline–McClintock procedure [20]).

Also shown in Fig. 2 are the results of Spalding and Chi [21], Simpson *et al.* [22], Andersen *et al.* [23] and Depooter [19]. A brief comparison of results is enough to see the difficulties in estimating wall shear stress accurately. The results of Simpson *et al.* and Andersen *et al.* are chosen here for comparison since their experimental rig is one of the few built to comparative tolerances as that of the present study. The porous plates of the present test section are claimed to have a lateral permeability variation of $\pm 2\%$ [15] and that of the Stanford rig is $\pm 6\%$ [2].

The present results fall well within the range of uncertainty as determined by the comparative data and appear to be consistent over the range of V_w^* studied.

3.2. *Mean profiles and velocity correlations*

The general behaviour of the mean profile data over the range of blowing is consistent with that of other workers [22, 23]. Specific profiles will not be given here and the reader is referred to Table 1 for the summary data of the relative integral parameters.

It has been suggested that a convenient and universal method of plotting velocity profiles is to use the parameter

$$\psi^+ = \frac{2U^+}{(1 + V_w^+ U^+)^{1.2} + 1}. \tag{1}$$

This parameter has been useful in studying the "universal" character of velocity profiles in the log-law and wake portions of the boundary layer. Integration of the appropriate Couette flow equations, with neglect of the viscous shear term and the substitution of $l_m^+ = \kappa y^+$ leads to the following equation for ψ^+ [24];

$$\psi^+ = \frac{1}{\kappa} \ln y^+ + f(V_w^+) + C. \tag{2}$$

Here $f(V_w^+)$ is chosen such that it is equal to zero for $V_w^+ = 0$ and equation (2) reduces to the "law of the wall". This form of the equation is usually considered valid in the fully turbulent portion of the inner region of a boundary layer, which is termed the "logarithmic region". Plots of the present profiles in $\psi^+ - y^+$ coordinates indicate that f is a very weak function of V_w^+ at low to medium transpiration rates. The data also seem to indicate that $f(V_w^+)$ is a monotone

Table 1. Experimental measurements: integral parameters of the boundary layer

Run No.	V_w^* ($\times 10^3$)	Re_x ($\times 10^{-6}$)	Re_{δ_2} ($\times 10^{-3}$)	C_f ($\times 10^3$)	u_τ [m/s]	V_w^+	B	T_B^+	x^+ ($\times 10^{-4}$)	δ [cm]	δ_1^* ($\times 10^{-3}$)	H	Δ_1^+ ($\times 10^{-3}$)	Δ_2^+ ($\times 10^{-4}$)	G
120777.02	0	0.63	1.49	3.79	0.45	0	0	144	2.75	2.07	2.11	1.42	1.98	1.34	6.77
120777.01	0	1.27	2.72	3.34	0.85	0	0	187	5.20	1.93	3.80	1.40	3.56	2.47	6.93
110777.01	0	2.06	3.71	3.05	0.80	0	0	240	8.06	2.77	5.11	1.38	4.76	3.24	6.81
110977.11	1.05	0.47	1.54	3.00	0.46	0.0272	0.702	174	1.82	1.71	2.33	1.51	2.20	1.91	8.71
110977.12	1.05	1.20	3.21	2.45	0.42	0.0301	0.860	174	4.21	3.52	4.71	1.47	4.45	4.03	9.05
080877.11	1.05	1.28	3.72	2.40	0.73	0.0304	0.877	185	4.45	2.42	5.35	1.44	5.03	4.41	8.76
090877.11	1.03	2.08	5.45	2.20	0.70	0.0310	0.935	161	6.90	3.45	7.86	1.44	7.41	6.80	9.17
130877.11	1.03	2.87	6.76	2.10	0.68	0.0319	0.984	164	9.29	4.25	9.55	1.41	9.00	8.09	8.98
160877.11	2.11	1.29	4.11	1.70	0.61	0.0725	2.49	219	3.78	2.57	6.41	1.56	6.08	7.45	12.3
160877.12	2.11	2.07	7.18	1.45	0.56	0.0785	2.92	241	5.56	4.17	10.9	1.51	10.3	12.99	12.5
140877.11	2.12	2.86	9.14	1.36	0.54	0.0812	3.11	361	7.44	5.39	13.5	1.48	12.8	15.9	12.4
180877.12	4.33	1.28	6.68	1.20	0.51	0.177	7.23	360	3.13	3.60	11.2	1.67	10.7	17.4	16.3
180877.11	4.33	2.06	10.4	0.93	0.46	0.201	9.32	299	4.45	5.50	17.2	1.65	16.5	29.8	18.1
180877.13	4.34	2.83	13.9	0.87	0.43	0.213	10.2	546	5.91	7.33	22.5	1.62	21.6	39.3	18.2
300877.12	6.23	1.27	9.12	0.63	0.37	0.351	19.8	284	2.26	4.68	17.1	1.88	16.5	43.2	26.2
300877.13	6.23	2.06	14.4	0.39	0.29	0.446	31.9	243	2.88	7.28	26.3	1.83	25.4	81.7	32.2
300877.11	6.23	2.85	19.8	0.32	0.26	0.493	39.0	248	3.61	9.62	36.3	1.83	35.1	125	35.7
290877.11	8.55	1.27	11.7	0.13	0.17	1.06	131	68	1.02	5.83	24.3	2.08	23.5	151	64.2
290877.12	8.57	2.83	24.8	0.05	0.10	1.72	343	43	1.41	12.1	47.2	1.90	46.7	424	92.8

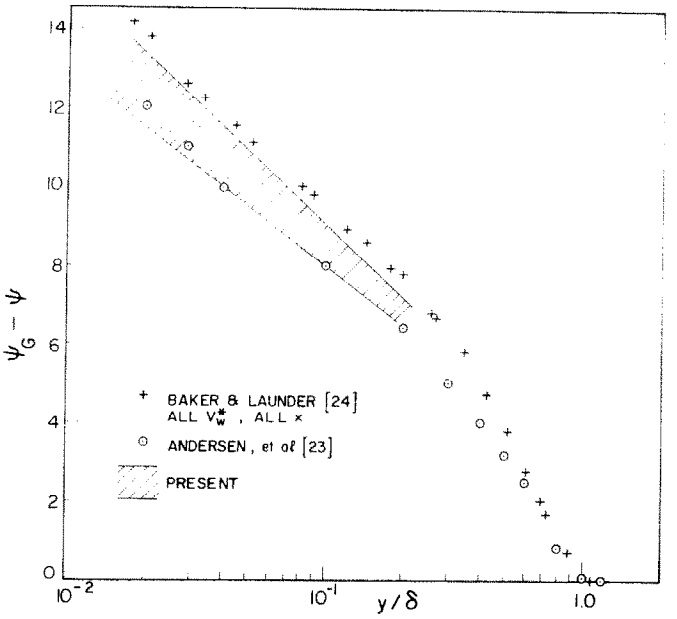

FIG. 3. Form of the velocity defect profiles, $\psi_G^+ - \psi^+$ vs y/δ.

decreasing function up to $V_w^+ \sim 0.5$, which is consistent with earlier findings [24]. For $V_w^+ > 0.5$ (i.e. the highest blowing fraction considered in the present study) considerable variation of V_w^+ can be observed for constant V_w^* and this is also reflected upon $f(V_w^+)$. It was noted that $f(V_w^+)$ does not seem to be a wholly monotone decreasing function with V_w^+, but that it actually increases in this latter range of transpiration. Any suggestion here however must be highly tentative due to the large uncertainty in measured wall shear stress. The functional form of $f(V_w^+)$ is not pursued here further since recent computational trends indicate that numerical integration of the fundamental equations is favoured more than the "universal law of wall" arguments. The reason for this is the interest in more complex flows which necessitate the introduction of the effects of turbulence fine structure into physical models described by differential equations and advances in computational techniques.

Figure 3 shows the form of the velocity profiles plotted in velocity defect form $\psi_G^+ - \psi^+$. This form makes the profiles independent of $f(V_w^+)$, as also has been pointed out by Coles [25] and Baker and Launder [24]. All the profiles from the present study as well as the ones from Simpson *et al.* considered here for comparison fall within the band plotted in the figure.

The general behaviour of turbulence intensities, turbulent shear stress and turbulent kinetic energy in the transpired boundary layer with constant V_w^* are displayed in Figs. 4–6. More detailed data can be found in Alp [18].

In Fig. 4 the turbulence intensity in the mainstream direction, $(\overline{u^2})^{1/2}/u_\tau$ is presented for all V_w^* at the highest Re_x investigated in the present study. In general, the level increases with higher blowing and the location of the maximum moves further away into the boundary layer. The latter observation indicates that

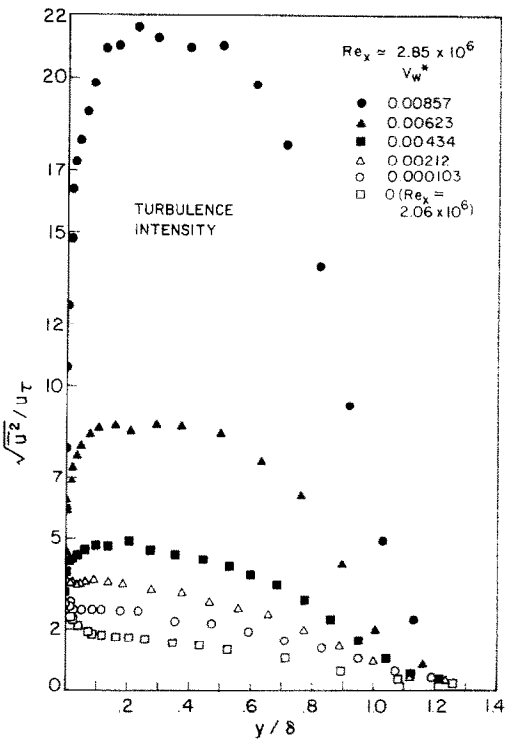

FIG. 4. Turbulence intensity, $(\overline{u^2})^{1/2}/u_\tau$ vs y/δ, at constant Re_x.

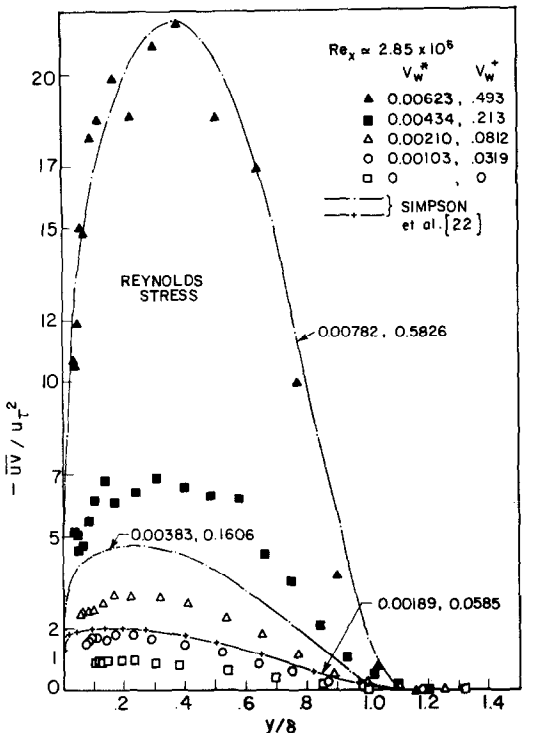

FIG. 5. Reynolds stress, $-\overline{uv}/u_\tau^2$ vs y/δ, at constant Re_x.

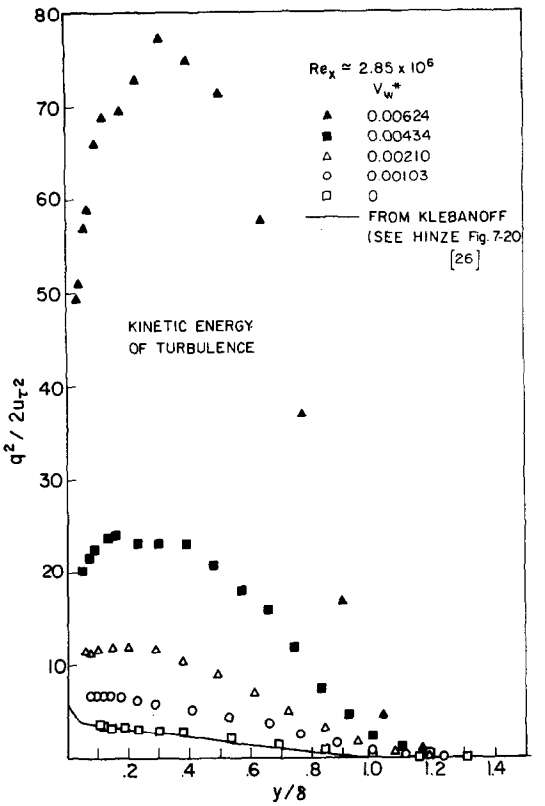

FIG. 6. Kinetic energy of turbulence, $q^2/(2u_\tau^2)$ vs y/δ, at constant Re_x.

with blowing, a larger portion of the boundary layer comes under the influence of "wall phenomena".

The same general trend can be observed for the shear stress $-(\overline{uv}/u_\tau^2)$ (Fig. 5) and the kinetic energy $q^2/2u_\tau^2$ (Fig. 6). Figure 5 also shows some shear stress profiles reported by Simpson *et al.* [22]. They were generated from experimentally measured velocity pro-

Table 2. Experimental measurements: characteristic time scales

Run No.	V_w^*	Re_x	Re_{δ_2}	T_B [s] ($\times 10^3$)	T_B^+	V_w^+	$T_B^* = \frac{T_B U_G}{\delta_1}$	$\bar{T}_B$
120777.02	0	6.31×10^5	1486	11.5	144	0	35.6	0
120777.01	0	1.27×10^6	2720	4.25	187	0	29.5	0
110777.01	0	2.06×10^6	3711	6.02	240	0	30.1	0
110977.11	0.00105	4.71×10^5	1542	12.9	174	0.0272	50.0	0.129
110977.12	0.00105	1.20×10^6	3210	15.9	174	0.0301	30.2	0.158
080877.11	0.00105	1.28×10^6	3720	5.7	185	0.0304	28.8	0.171
090877.11	0.00103	2.08×10^6	5452	5.4	161	0.0310	18.7	0.155
130877.11	0.00103	2.87×10^6	6758	5.8	164	0.0319	16.4	0.167
160877.11	0.00211	1.29×10^6	4108	9.6	219	0.0725	40.2	1.151
160877.12	0.00211	2.07×10^6	7184	12.4	241	0.0785	30.7	1.485
140877.11	0.00212	2.86×10^6	9136	19.9	361	0.0812	39.3	2.380
180877.12	0.00433	1.28×10^6	6684	22.7	360	0.177	54.0	11.28
180877.11	0.00433	2.06×10^6	10432	24.2	299	0.210	37.4	12.08
180877.13	0.00434	2.83×10^6	13870	47.7	546	0.213	55.8	24.77
300877.12	0.00623	1.27×10^6	9121	34.1	284	0.351	52.8	34.99
300877.13	0.00623	2.06×10^6	14400	47.2	243	0.466	47.4	48.34
300877.11	0.00623	2.85×10^6	19807	58.7	248	0.493	42.8	60.28
290877.11	0.00855	1.27×10^6	11675	42.0	68	1.060	45.7	76.40
290877.12	0.00857	2.83×10^6	24800	66.0	43	1.715	36.0	126.47

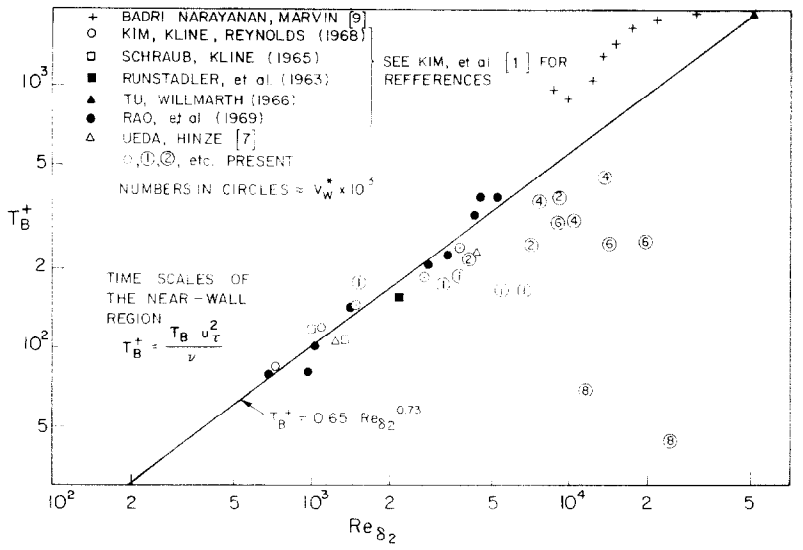

FIG. 7. Time scales of the near-wall region; T_B^+ vs Re_{δ_2}.

files and wall shear stress using an integrated form of the x-momentum and continuity equations. The agreement with the present data is seen to be quite good. The uncertainty in the measurement of $\overline{uv}$ is estimated to be nominally $\pm 5\%$ over most of the traverse but higher near the wall due to uncertainties in hot-wire calibration at low velocities.

3.3. *Time scales of the near-wall layer*

The results of the experimental investigation on the unsteady behaviour of the flow near a porous wall are presented in Table 2. A characteristic mean period of activity, T_B, was measured as a function of transpiration and Reynolds number in a zero pressure gradient boundary layer. Figures 7–10 summarize these results.

In Fig. 7, the parameter $T_B^+ = (T_B u_\tau^2/\nu)$ is plotted against the momentum thickness Reynolds number, Re_{δ_2}. This figure also contains data of some earlier studies for flows with no transpiration. The straight line is the correlation given by Rao *et al.* [5]. Zero transpiration data, although rather scattered, seem to be correlated well by the given line. However, when blowing occurs, no systematic variation of T_B^+ with Re_{δ_2} or transpiration can be observed. It should be noted that the scatter is well within the $\pm 73\%$ uncertainty interval (computed by the Kline, McClintock procedure) accompanying these data points. It

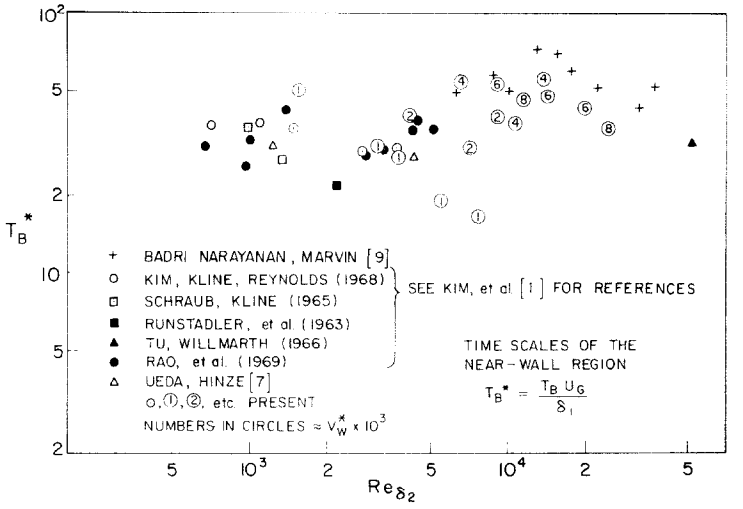

FIG. 8. Time scales of the near-wall region; T_B^* vs Re_{δ_2}.

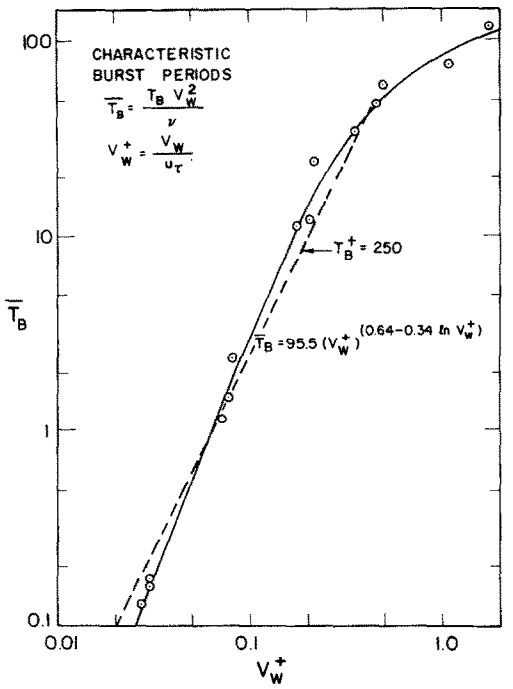

FIG. 9. Time scales of the near-wall region; $\bar{T}_B$ vs V_w^+.

also seems that the large scale turbulence structure in the inner layer of a boundary layer thickened by high rates of blowing is not the same as that of a flat plate boundary layer which simply has a high momentum thickness Reynolds number. Implicit in this statement is the assumption that T_B^+ is the appropriate time scale of large scale turbulence structure in the sublayer.

A more interesting behaviour is observed when $T_B^* = (T_B U_G/\delta_1)$ is plotted against Re_{δ_2} (Fig. 8). In spite of the high scatter of the data, the general behaviour seems to be that T_B^* is a constant at a value of about 35, and does not vary significantly with Re_{δ_2}. This confirms the belief that large scale fluctuations of the outer layer correlate well with large scale fluctuations of the inner layer [9, 26] and that the large scale behaviour of the boundary layer is not a strong function of the momentum thickness Reynolds number. No systematic variation of T_B^* with blowing can be seen.

The characteristic velocities used above in the non-dimensional groups are the free stream velocity U_G and the friction velocity u_τ. These are the only velocity scales one encounters in non-transpired (including cases of non-zero pressure gradient) boundary layers. However, in a transpired boundary layer there is another characteristic velocity which can be used in dimensionless groups, namely, the transpiration velocity V_w. This velocity, it turns out, is very convenient in expressing time scale data.

Figure 9 shows the variation of $\bar{T}_B = (T_B V_w^2/\nu)$ with $V_w^+ = V_w/u_\tau$. All the points fall close to a single curve. V_w^+ includes the effects of Reynolds number through u_τ. The solid curve can be represented by the equation:

$$\bar{T}_B = 95.5\,(V_w^+)^{(0.64-0.34\ln V_w^+)} \qquad 0.03 < V_w^+ < 1.72$$

or

$$V_w^+ = 2.53\exp[-1.70(4.86 - \ln \bar{T}_B)^{1/2}$$
$$0.1 < \bar{T}_B < 129$$

which was obtained by a least squares fit to data. It should be emphasized here, that the functional form used in the correlation is merely a convenient way of representing data with a single equation. In the range $V_w^+ = 0.5$, the data points lie very close to the straight line $\bar{T}_B \simeq 250 V_w^{+2}$ or $T_B^+ \simeq 250$, i.e. T_B^+ is only a weak function of V_w^+. However, the dependence seems to be real when the straight line $T_B^+ = 250$ is considered together with the present data as plotted in Fig. 10. The weak dependence of T_B^+ on V_w^+ for $0.03 < V_w^+ < 0.5$, the broad maximum around $V_w^+ \sim 0.25$ and the sudden decrease for large V_w^+, all seem to be coincident with the inverse behaviour of $f(V_w^+)$ in the "law of the wall" for transpired flows as briefly

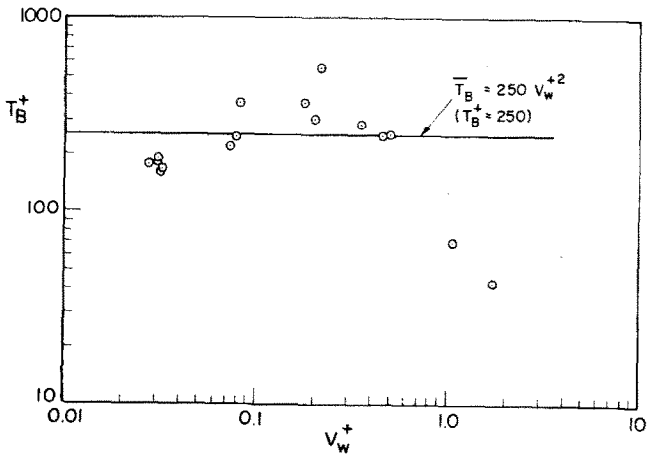

FIG. 10. Time scales of the near-wall region; T_B^+ vs V_w^+.

mentioned earlier in Section 3.2.

4. CONCLUSIONS

An experimental investigation of the wall region of a boundary layer with blowing was made and a characteristic time scale T_B was measured.

T_B is found to increase both with blowing and Reynolds number. For a given free stream velocity U_G, the boundary-layer thickness δ also increases. This observation has two immediate implications, namely, that the inner layer time scale T_B correlates with an outer layer parameter such as δ, and also that T_B is probably an inverse function of the overall velocity gradient U_G/δ. Figure 8 confirms this idea. This statement is not meant to imply that T_B is necessarily the dependent parameter in the functional relationship.

The present results indicate that one can correlate the time scale T_B with the independent parameters of the flow using

$$\bar{T}_B = \frac{T_B V_w^2}{\nu}$$

and

$$V_w^+ = \frac{V_w}{u_\tau}$$

as the dimensionless parameters.

Further work has shown that, when the empirical correlation as given in Section 3 is used in conjunction with a "mixing length" model suitably modified to incorporate a time scale of the viscous sublayer, it can successfully predict velocity profiles, Alp *et al.* [27]. This mixing length model was developed by simulating the unsteady behaviour of the near-wall regions through a modified van Driest type damping function. The damping function, the form of which was derived analytically, contained a parameter relating to the period of the unsteady behaviour, non-dimensionalized in the same way as $\bar{T}_B$. This parameter was replaced by the above empirical correlation in order to close the equations for the prediction of velocity profiles thus rendering the mixing length a function of V_w^+ only. The two dimensionless parameters $\bar{T}_B$ and V_w^+ hence proved to be convenient parameters for use with this mathematical model.

The mean velocity profiles have been shown to be well characterized by the functional form $U^+(y^+, V_w^+)$ with the effect of blowing more pronounced in the wake region than in the "logarithmic" region [18].

Examination of the profiles of turbulence parameters show that the location of maximum intensity of fluctuations is shifted further away from the wall with increasing blowing. This indicates an increase in the length scale of fluctuations near the wall since the "activity" is no more "squeezed" into a very small region. The magnitude of fluctuations scaled with free stream velocity also increases with blowing, but only slowly. These two observations, when coupled together, indicate an increase in the time scale T_B of the near-wall region, which is consistent with the present experimental findings of T_B.

Furthermore, the variation of the parameter T_B^+ with the transpiration parameter V_w^+ seems to coincide with the inverse behaviour of $f(V_w^+)$, which has been used in the "law of the wall" studies of the transpired turbulent boundary layer.

Acknowledgement — The authors gratefully acknowledge the invaluable discussions provided by the late Professor W. B. Nicoll during the course of this work. Support for this work from the Natural Sciences and Engineering Research Council of Canada (NSERC) is also gratefully acknowledged.

REFERENCES

1. H. T. Kim, S. J. Kline and W. C. Reynolds, The production of turbulence near a smooth wall in a turbulent boundary layer, *J. Fluid Mech.* **50,** 133–160 (1971).
2. W. M. Kays and R. J. Moffatt, The behaviour of transpired turbulent boundary layers, HMT-20, Stanford University (1975).
3. S. J. Kline, W. C. Reynolds, F. A. Schraub and P. W. Runstadler, The structure of turbulent boundary layers, *J. Fluid Mech.* **30,** 741–773 (1967).
4. E. R. Corino and R. S. Brodkey, A visual investigation of the wall region in turbulent flow, *J. Fluid Mech.* **37,** 1–30 (1969).
5. K. N. Rao, R. Narasimha and M. A. Badri Narayanan, The 'bursting' phenomenon in a turbulent boundary layer, *J. Fluid Mech.* **48,** 339–352 (1971).
6. S. S. Lu and W. W. Willmarth, Measurements of the structure of the Reynolds stress in a turbulent boundary layer, *J. Fluid Mech.* **60,** 481–511 (1973).
7. H. Ueda and J. O. Hinze, Fine-structure turbulence in the wall region of a turbulent boundary layer, *J. Fluid Mech.* **67,** 125–143 (1975).
8. T. R. Heidrick, S. Banerjee and R. S. Azad, Experiments on the structure of turbulence in fully developed pipe flow, part 2, *J. Fluid Mech.* **82,** 705–723 (1977).
9. M. A. Badri Narayanan and J. G. Marvin, On the period of the coherent structure in boundary layers at large Reynolds numbers, NASA TM78477 (1978).
10. S. V. Patankar, Wall shear stress and heat flux laws for turbulent boundary layers with a pressure gradient: use of Van Driest's eddy viscosity hypothesis, Imperial College, London, TWF/TN/14 (1966).
11. E. Brundrett, W. B. Nicoll and A. B. Strong, Heat and mass transfer in an incompressible turbulent boundary layer, *J. Heat Transfer* **7,** 23–28 (1972).
12. E. R. van Driest, On turbulent flow near a wall, *J. Aeronaut. Sci.* **23,** 1007–1011 (1956).
13. K. C. Watts, E. Brundrett, W. B. Nicoll and A. B. Strong, Mixing length distributions in the near-wall region of transpired turbulent boundary layers, *J. Fluid Engng* **96,** 301–313 (1974).
14. K. C. Watts, The development of asymptotic turbulent, transitional and laminar boundary layers induced by suction, Ph.D. Thesis, Dept. of Mech. Engng, Univ. of Waterloo (1972).
15. K. C. Watts, E. Brundrett, W. B. Nicoll and A. B. Strong, Design and construction of a wind tunnel for mass transfer studies in incompressible boundary layers, *J. Fluid Engng* **96,** 311–316 (1974).
16. K. Depooter, E. Brundrett and A. B. Strong, The calibration of Preston tubes in transpired turbulent boundary layers, *J. Fluid Engng* **100,** 10–16 (1978).
17. E. Brundrett and K. C. Watts, Simultaneous measurements of Reynolds stress and turbulent kinetic energy for two-dimensional boundary layers, *J. Fluid Engng* **97,** 112–113 (1975).

18. E. Alp, Measurements on a transpired turbulent boundary layer and a mixing-length model employing near-wall characteristic time scales, Ph.D. Thesis, University of Waterloo (1978).
19. K. Depooter, The measurement of wall shear stress on a porous plate with mass transfer using a floating element technique and the investigation of various indirect measuring methods, Ph.D. Thesis, University of Waterloo (1973).
20. S. J. Kline and F. A. McClintock, Describing uncertainties in single sample experiments, *Mech. Engng* **75**, 3–8 (1953).
21. D. B. Spalding and S. W. Chi, The drag of a compressible turbulent boundary layer on a smooth flat plate with and without heat transfer, *J. Fluid Mech.* **18**, 114–143 (1964).
22. R. L. Simpson, W. M. Kays and R. J. Moffatt, The turbulent boundary layer on a porous plate: an experimental study of the fluid dynamics with injection and suction, HMT-2, Stanford Univ. (1967).
23. P. S. Andersen, W. M. Kays and R. J. Moffatt, The turbulent boundary layer on a porous plate: an experimental study of the fluid mechanics for adverse free-stream pressure gradients, HMT-5, Stanford Univ. (1972).
24. R. J. Baker and B. E. Launder, The turbulent boundary layer with foreign gas injection—I. Measurements in zero pressure gradient, *Int. J. Heat Mass Transfer* **17**, 275–291 (1974).
25. D. Coles, A survey of data for turbulent boundary layers with mass transfer, AGARD-CP-93 (1972).
26. J. O. Hinze, *Turbulence*, 2nd ed. McGraw-Hill, New York (1975).
27. E. Alp, A. B. Strong and W. B. Nicoll, A near-wall turbulence model for transpired flow, in *Proceedings of the NATO Advanced Study Institute on Turbulent Forced Convection in Channels and Rod Bundles*, edited by S. Kacak and D. B. Spalding, Vol. 1, pp. 475–490. Hemisphere, New York (1979).

MESURES DES ECHELLES DE TEMPS CARACTERISTIQUES DE LA COUCHE LIMITE TURBULENTE AVEC TRANSFERT DE MASSE

Résumé — On présente les résultats sur une étude expérimentale de la couche limite turbulente avec transpiration, à pression et fraction de soufflage constants. Le fluide en mouvement est de l'air à pression atmosphérique. On mesure des échelles de temps caractéristiques de la région proche de la paroi, ainsi que des profils de vitesse moyenne et des paramètres de turbulence, à l'aide d'un anémomètre à fil chaud à température constante. On présente aussi des paramètres intégraux de la couche limite et des coefficients de frottement locaux. Des comparaisons sont faites avec des études antérieures.

La portion externe des profils de vitesse moyenne $U^+(y^+)$ semble être plus affectée par le soufflage que la portion proche de la paroi. La région de fluctuations maximales turbulentes s'éloigne de la surface quand le soufflage augmente, indiquant que l'échelle de temps des fluctuations près de la paroi grandit. Ceci est compatible avec les résultats sur l'échelle caractéristique de temps T_B. Le paramètre T_B est trouvé en bonne corrélation avec le paramètre de transfert massique V_w^+.

MESSUNGEN CHARAKTERISTISCHER ZEITMASSSTÄBE DER TURBULENTEN GRENZSCHICHT MIT STOFFTRANSPORT

Zusammenfassung—Es wird über die Ergebnisse einer experimentellen Untersuchung der turbulenten Grenzschicht bei Schwitzkülung mit konstantem Druck- und Einblasverhältnis berichtet. Das Arbeitsmedium war luft bei Umgebungsdruck. Sowohl die charakteristischen Zeitmaßstäbe des wandnahen Bereichs, als auch die Profile der mittleren Geschwindigkeit und die Turbulenzparameter wurden mittels Konstanttemperatur-Hitzdrahtanemometrie bestimmt. Integrale Grenzschichtparameter und lokale Widerstandszahlen werden dargestellt und mit früheren Untersuchungen verglichen.

Der äußere Bereich der Profile der mittleren Geschwindigkeit $U^+(y^+)$ scheint durch die Einblasung stärker beeinflußt zu werden als der wandnahe Bereich. Das Gebiet der maximalen Turbulenzschwankungen bewegt sich bei Einblasung von der Wand weg, woraus geschlossen werden kann, daß der Längen- und damit der Zeitmaßstab der Schwankungen in Wandnähe vergrößert wird, was mit den Erkenntnissen über den charakteristischen Zeitmaßstab T_B übereinstimmt. Es hat sich gezeigt, daß der Zeitmaßstab $\bar{T}_B$ und der Stofftransportparameter V_w^+ einander gut zugeordnet werden können.

ИЗМЕРЕНИЕ ВРЕМЕННЫХ МАСШТАБОВ ТУРБУЛЕНТНОСТИ В ПОГРАНИЧНОМ СЛОЕ ПРИ НАЛИЧИИ МАССОПЕРЕНОСА

Аннотация — Представлены результаты экспериментального исследования турбулентного пограничного слоя со вдувом при постоянном давлении. Рабочей средой служил воздух при атмосферном давлении. Термоанемометром постоянной температуры измерялись временные масштабы турбулентности в области у стенки, а также профили средней скорости и параметры турбулентности. Кроме того приведены интегральные параметры пограничного слоя и локальные коэффициенты трения. Дано сравнение с данными предыдущих исследований. Показано, что вдув оказывает большее влияние на профили средней скорости $U^+(y^+)$ вдали от стенки, чем в пристеночной области. При вдуве область максимальных флуктуаций турбулентности отходит от стенки, свидетельствуя о том, что масштаб длины и, следовательно, временной масштаб флуктуаций у стенки возрастают. Это подтверждается данными по временному масштабу T_B. Найдено, что параметр временного масштаба $\bar{T}_B$ хорошо согласуется с параметром массопереноса V_w^+.